

# A table-top ultrashort light source in the extreme ultraviolet for circular dichroism experiments

A. Ferré<sup>1</sup>, C. Handschin<sup>1</sup>, M. Dumergue<sup>1</sup>, F. Burgy<sup>1</sup>, A. Comby<sup>1</sup>, D. Descamps<sup>1</sup>, B. Fabre<sup>1</sup>, G. A. Garcia<sup>2</sup>, R. Gêneaux<sup>3</sup>, L. Merceron<sup>1</sup>, E. Mével<sup>1</sup>, L. Nahon<sup>2</sup>, S. Petit<sup>1</sup>, B. Pons<sup>1</sup>, D. Staedter<sup>4</sup>, S. Weber<sup>3</sup>, T. Ruchon<sup>3</sup>, V. Blanchet<sup>1</sup> and Y. Mairesse<sup>1\*</sup>

**Circular dichroism in the extreme ultraviolet range is broadly used as a sensitive structural probe of matter, from the molecular photoionization of chiral species<sup>1–3</sup> to the magnetic properties of solids<sup>4</sup>. Extending such techniques to the dynamical regime has been a long-standing quest of solid-state physics and physical chemistry, and was only achieved very recently<sup>5</sup> thanks to the development of femtosecond circular extreme ultraviolet sources. Only a few large facilities, such as femtoseconded synchrotrons<sup>6,7</sup> or free-electron lasers<sup>8</sup>, are currently able to produce such pulses. Here, we propose a new compact and accessible alternative solution: resonant high-order harmonic generation of an elliptical laser pulse. We show that this process, based on a simple optical set-up, delivers bright, coherent, ultrashort, quasi-circular pulses in the extreme ultraviolet. We use this source to measure photoelectron circular dichroism on chiral molecules, opening the route to table-top time-resolved femtosecond and attosecond chiroptical experiments.**

High-order harmonic generation (HHG) is an extremely non-linear optical process that occurs when an intense femtosecond light pulse interacts with a gaseous target. Many characteristics of the high-harmonic radiation make it a unique and ideal source for time-resolved studies, including small size, low cost, good spatial coherence<sup>9</sup>, brightness<sup>10</sup>, tunability<sup>11</sup> and ultrashort pulse duration (femtosecond<sup>12</sup> to attosecond<sup>13</sup>). HHG is thus being increasingly used as a light source for atomic<sup>14</sup>, molecular<sup>15,16</sup>, surface and solid-state<sup>17</sup> time-resolved spectroscopy.

HHG is generally achieved in rare gases using linearly polarized laser fields, yielding linearly polarized extreme ultraviolet (XUV) radiation, parallel to the fundamental polarization. When interacting with matter, such a radiation simply defines an axis. By contrast, circular polarized light (CPL) defines an orientation of space and is thus a unique probe of chiral matter. As such, its production is becoming a requested figure of merit of short-wavelength sources, especially in the 10–30 eV range, close to the ionization thresholds of most molecular systems.

Converting a linearly polarized harmonic beam to circular polarization can be achieved using multiple reflections on surfaces, which have a different complex reflectivity of S and P polarization and induce a phase shift between these two components<sup>18</sup>. Such a set-up reduces the photon flux by two orders of magnitude. The direct generation of circular harmonics with high efficiency is thus preferable for practical applications. Although the most natural way to generate CPL from high harmonics would seem at first sight to be to use a circularly polarized fundamental laser pulse, the harmonic emission decreases exponentially with laser

ellipticity<sup>19</sup>, which imposes severe restrictions on the range of usable ellipticities. The ellipticity of the harmonic radiation in rare gases being generally lower than that of the driving laser, an efficient generation of XUV pulses with ellipticities above 20% is precluded<sup>20</sup>. The only reported exception to this rule is harmonic 17 from neon<sup>20</sup>, which is characterized by higher ellipticity but a very low generation efficiency.

Using additional electric or magnetic fields can counteract the decay of the harmonic signal with ellipticity, enabling HHG from quasi-circular laser pulses<sup>21,22</sup>. Fleischer *et al.* recently demonstrated the ellipticity control of harmonics using a combination of circularly polarized 800 nm and 410 nm pulses<sup>23</sup>. They were able to produce a spectrum consisting of double peaks with alternately left and right circular polarization. This method is interesting because it provides a universal way of generating circular XUV photons with good efficiency. It is particularly appropriate for XUV magnetic circular dichroism experiments, which rely on the measurement of absorption spectra. Nevertheless, this source is not the most appropriate for photoionization of polyatomic molecules, in which each spectral peak produces a broad photoelectron spectrum associated with different cationic states with different ionization dynamics. The overlap of photoelectron spectra from spectrally shifted left and right CPL would make analysis quite complex. Furthermore, on the attosecond timescale this source produces trains of linearly polarized attosecond pulses with alternating polarization direction, and cannot be used for attosecond circular dichroism.

An alternative solution for the generation of elliptical harmonics emerged a few years ago in the form of molecular HHG<sup>24–26</sup>. It was shown that the ellipticity of high harmonics may reach 40% in nitrogen molecules aligned at 60° from the polarization direction of linear generating laser pulses<sup>25,26</sup>. Although this method may provide brighter sources, it is quite cumbersome to implement because of the equipment required to efficiently align molecular samples.

In addition to their rather low efficiency and/or relative complexity, the elliptical HHG experiments reported to date have been unable to unambiguously prove the existence of circular harmonic emission, as they could not distinguish unpolarized radiation from circular radiation<sup>20</sup>. This questions the actual value of the ellipticity and the possibility of using such elliptical sources in practical applications.

In this Letter, we show that resonant HHG in elliptical laser fields provides a unique source of quasi-circular XUV radiation within a simple optical set-up. We demonstrate the influence of resonances on the high-harmonic ellipticity by studying the simple case of argon. Using an XUV polarizer, we find that harmonic 5 from a

<sup>1</sup>Université de Bordeaux – CNRS – CEA, CELIA, UMR5107, F33405 Talence, France. <sup>2</sup>Synchrotron SOLEIL, l'Orme des Merisiers, Saint Aubin BP 48, 91192 Gif sur Yvette Cedex, France. <sup>3</sup>CEA, IRAMIS, Lasers, Interactions and Dynamics Laboratory – LIDyL, CEA-SACLAY, F-91191 Gif-sur-Yvette, France.

<sup>4</sup>Université de Toulouse – CNRS, LCAR-IRSAMC, Toulouse, France. \*e-mail: mairesse@celia.u-bordeaux1.fr

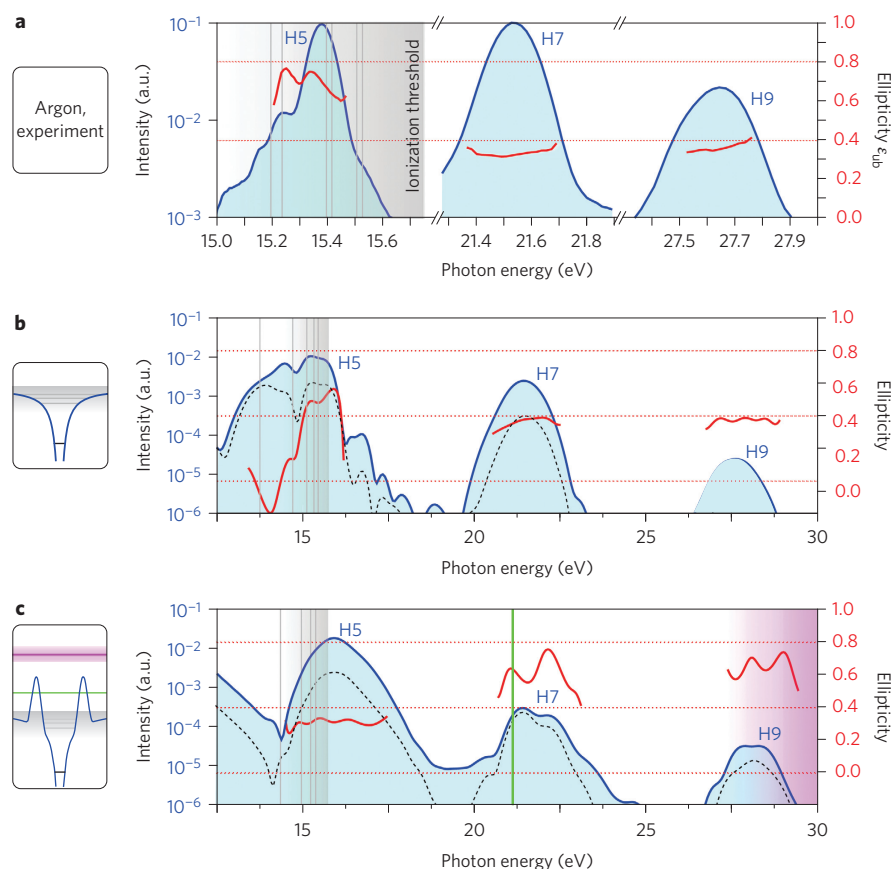


**Figure 1 | Elliptical resonant HHG in argon.** **a**, Experimental harmonic intensity (blue area, log-scale) and upper-bound ellipticity (red continuous line) generated using 404 nm,  $\sim 1 \times 10^{14}$  W cm $^{-2}$  pulses with  $\epsilon_0 = 0.4$ . Thin grey vertical lines indicate positions of resonances. a.u., arbitrary units. **b**, Theoretical results at 400 nm,  $\sim 1 \times 10^{14}$  W cm $^{-2}$ ,  $\epsilon_0 = 0.4$ , using a soft-core Coulomb potential. The thin dashed black line shows the orthogonal component of the harmonic emission. **c**, Theoretical results using a modified potential with a shape resonance around 21 eV (green vertical line) and a broad resonance in the continuum from 27 to 36 eV (purple area).

404 nm pulse with  $\epsilon_0 = 40\%$  ellipticity reaches 75% ellipticity. A theoretical study shows that this effect is due to the presence of resonances below the ionization threshold. This study also indicates that continuum resonances, above the ionization threshold, also lead to highly elliptical harmonics. To extend the spectral range of elliptical XUV emission, we changed the generation gas for SF $_6$ , a molecular system with a high ionization potential (15.7 eV) and a rich ionization continuum involving several resonances<sup>27,28</sup>. Optical polarimetry confirmed the existence of high ellipticity in a broad spectral region. The quality of this elliptical femtosecond XUV source enabled us to induce macroscopic asymmetries in the one-photon ionization of pure enantiomers of randomly oriented fenchone molecules, via the so-called photo-electron circular dichroism (PECD) process<sup>2</sup>.

To study resonant HHG by elliptical laser fields we generated harmonics of 404 nm pulses in argon. Details about the experiment are provided in the Methods. Harmonic 5 is centred at 15.3 eV, just below the ionization potential of Ar (15.76 eV). Figure 1a shows the harmonic spectrum obtained using fundamental pulses with  $\epsilon_0 = 0.4$  ellipticity. Although the harmonics generated above the ionization threshold have a smooth Gaussian-like spectral profile, harmonic 5 is spectrally narrower and shows additional structures. Such spectral structuring of below-threshold harmonics has recently been identified as the signature of resonant bound-bound transitions in HHG<sup>29</sup>.

Measuring light polarization requires a rotating polarizer, which modulates the intensity following the Malus' law<sup>30</sup>. This enables the polarization direction of the linear component of the radiation to be

determined, but is not enough to measure the circular polarization rate  $S_3$  because of the possible presence of unpolarized radiation ( $S_4$ ), where  $S_i$  are the conventional Stokes parameters. As such, the Malus' law provides an upper bound of the ellipticity,  $\epsilon_{ub} = \sqrt{[1 - (S_1^2 + S_2^2)]}$ . In our experiment, a fixed polarizer was used and the harmonic spectrum was recorded as a function of the rotation of the laser's main axis of polarization.  $\epsilon_{ub}$  was extracted by Fourier transform of the XUV yield oscillations, for each component of the harmonic spectrum. The results are shown in Fig. 1a. Above the ionization threshold the ellipticity is slightly lower than that of the driving laser, and rather uniform over the spectral width of each harmonic. By contrast, harmonic 5 shows a much higher ellipticity, reaching 0.77, with an oscillating behaviour.

To investigate the influence of bound-bound resonances on harmonic ellipticity, we performed a theoretical study based on the resolution of the time-dependent Schrödinger equation in two dimensions. Details for the calculations are provided in the Supplementary Information. Figure 1b shows the harmonic spectrum and ellipticity obtained using a soft-core Coulomb potential mimicking the ionization potential of Ar. Similar to the experiment, above-threshold harmonics have a regular spectral profile and an ellipticity slightly lower than the fundamental pulse, while harmonic 5 shows structures both in the spectrum and ellipticity. The ellipticity is higher than 0.4 above 15 eV and becomes negative at 14 eV. Calculations show that the values of the ellipticity in the resonant area strongly depend on the exact structure of the potential, so the agreement with the experiment can only be qualitative. The high values of the ellipticity are associated with an increase of the

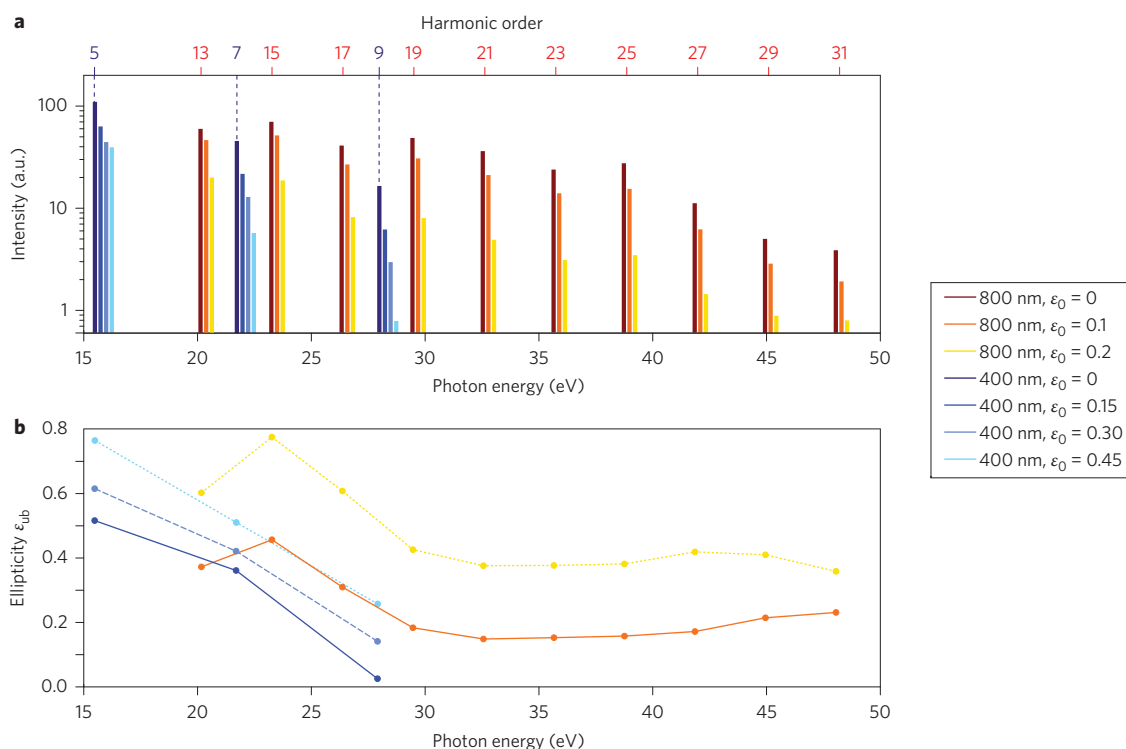


**Figure 2 | Optical polarimetry measurements of HHG in SF<sub>6</sub>.** **a**, Harmonic signal produced by 800 nm,  $1.3 \times 10^{14}$  W cm<sup>-2</sup> pulses (brown to yellow, harmonics 13 to 31), and by 400 nm,  $1 \times 10^{14}$  W cm<sup>-2</sup> pulses (dark to light blue, harmonics 5 to 9). a.u., arbitrary units. **b**, Ellipticity of the harmonic radiation (upper limit) determined using an XUV polarizer. The error on ellipticity measurements, determined by comparing consecutive measurements in identical conditions, is  $\pm 0.03$ .

orthogonal component of the harmonic emission under the influence of the resonance. These results demonstrate the role of bound-bound resonant transitions in the generation of highly elliptical harmonics.

Resonant below-threshold HHG holds great potential for creating circular XUV sources. It is very easy to implement, and is bright enough for applications in the gas phase. Using a calibrated photodiode we measured that this source produces  $7 \times 10^6$  photons per pulse for harmonic 5 when driven by 30% ellipticity; this can be extended to higher flux by increasing the generating pressure, without suffering from reabsorption like higher harmonics<sup>29</sup>. On the other hand, it is restricted to low photon energies, below the ionization potential of the gases conventionally used for intense HHG (argon, 15.76 eV; krypton, 14 eV; xenon, 12.13 eV). Can quasi-circular harmonics also be generated using resonances lying above the ionization threshold? To answer that question we modified the potential used in our calculations. We added a potential barrier that creates a shape resonance in the continuum, around the energy of harmonic 7. Such shape resonances are very common in ionization spectra of molecules in the 10–20 eV range above the ionization threshold. The modification of the potential also created another resonance, much broader in energy and higher in the continuum (from 27 eV to 36 eV). The dipole moments associated with these resonances are shown in the Supplementary Information. The results shown in Fig. 1c indicate that continuum resonances boost the orthogonal component of the harmonic emission, giving ellipticities of H7 and H9 of up to 0.75.

The simulations demonstrate the generality of quasi-circular HHG by different types of resonances, opening a path to the generation of highly elliptical XUV pulses over a broad spectral range, at higher photon energies. To validate this idea and design the ideal source for applications we chose SF<sub>6</sub> as a generating medium. We recently conducted high-harmonic spectroscopic studies of this

molecule<sup>28</sup>, which revealed that the harmonic emission in the 20–25 eV range was dominated by a shape resonance in the A ionization channel (associated with the first excited state of the cation)<sup>27</sup>. Figure 2 shows the harmonic intensity and ellipticity produced in SF<sub>6</sub> using 800 nm pulses. Ellipticity  $\epsilon_{ub}$  reaches unprecedented values (between 60 and 80% for a fundamental ellipticity of only 20%) between harmonics 13 and 17 (20–27 eV). This is in agreement with the position of the shape resonance. A secondary maximum in the ellipticity around 45 eV could also be due to resonances in the A/B channel at 35 eV and 49 eV (ref. 27).

We also performed additional characterization of the elliptical XUV radiation. The beam shows low divergence (2–4 mrad) and excellent spatial coherence properties; creating two harmonic sources spatially shifted by  $\sim 100$   $\mu$ m results in a nice Young's slits interference pattern with high contrast ( $\sim 60\%$  visibility). This ensures a good focusability of the elliptically polarized harmonics, which could be crucial for further applications. The spectral width of harmonics 13 to 17 is  $\sim 150$  meV full-width at half-maximum. The ultrashort character of the harmonic emission was checked by initiating molecular vibrations in SF<sub>6</sub>, which modulate the harmonic yield with a 43 fs period<sup>31</sup>, indicating that the emission is shorter than this period.

The generation of a dense frequency comb with  $\sim 3$  eV step (HHG at 800 nm) can be problematic in studying the photoionization of polyatomic molecules with congested spectra. This issue can be circumvented by increasing the spacing between consecutive harmonics, using a shorter-wavelength fundamental pulse. The results obtained using 400 nm fundamental pulses, which lead to a 6.2 eV step in the harmonic comb, are shown in Fig. 2. The decay of the harmonic efficiency with ellipticity is less important, in particular for harmonic 5, enabling the use of higher  $\epsilon_0$ . The harmonic maximum ellipticities still reach very high values: almost 80% for harmonic 5 (15.5 eV) and 50% for harmonic 7 (21.7 eV) with

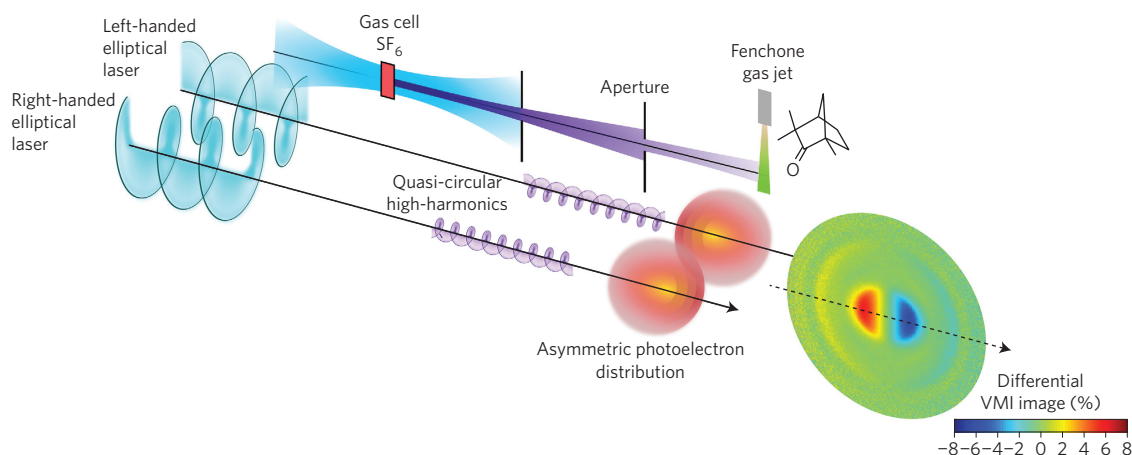


**Figure 3 | Experimental set-up and principle of the PECD measurement.** Left- and right-handed elliptical 400 nm pulses are used alternately to generate high harmonics in SF<sub>6</sub>. An aperture selects the central part (2 mm diameter) of the harmonic beam, which photoionizes enantiopure fenchone molecules in a VMIS. The photoionization of chiral molecules results in asymmetric forward/backward photoelectron emission. This asymmetry appears clearly in the differential photoelectron image (corresponding to fenchone (+)), which is the normalized difference between the electron images obtained using left- and right-handed fundamental pulses:  $2(S_{\text{left}} - S_{\text{right}})/(S_{\text{left}} + S_{\text{right}})$ .

$\varepsilon_0 = 45\%$ . Using shorter wavelengths for HHG also has the advantage of increasing the generation efficiency<sup>32</sup>. We measured  $2 \times 10^6$  photons per pulse for harmonic 5 when driven by 30% ellipticity, that is,  $2 \times 10^9$  photons per second. This is lower than the  $\sim 1 \times 10^{12}$  photons per second of a quasi-continuous synchrotron beamline such as DESIRS, but still permits pump-probe experiments on dilute matter to be performed. The photon flux could be further increased by optimizing the generating conditions (more energetic laser pulses, longer focal length) without any drastic change in the polarization quality.

As a test case to characterize our elliptical harmonic source, we performed a PECD experiment on a previously studied chiral system. PECD arises when circular radiation photoionizes pure enantiomers of a chiral molecule in the gas phase. The emitted electrons exhibit a large forward/backward asymmetry along the propagation direction of the light, even for randomly oriented molecular samples<sup>2</sup>. The harmonics of the 400 nm laser pulse were directly sent to a velocity map imaging spectrometer (VMIS) where they photoionized enantiopure chiral fenchone molecules (Fig. 3). To avoid modification of the XUV polarization state, no optical element was introduced between XUV generation and the VMIS. An aperture selected the central part of the harmonic beam to maintain good resolution in the VMIS. We checked that the fundamental beam was not intense enough in the detection zone to ionize the fenchone or produce two-photon two-colour transitions. The VMIS projects the angular distribution of ionized electrons onto a set of microchannel plates imaged by a charge-coupled device (CCD) camera. Photoelectron spectra were measured alternately using left-handed and right-handed driving laser ellipticities  $\varepsilon_0 = \pm 30\%$ . Calculating the normalized difference between the left and right images,  $\text{PECD} = 2(S_{\text{left}} - S_{\text{right}})/(S_{\text{left}} + S_{\text{right}})$ , provides a direct visualization of the dichroism in the measurement (as seen in Fig. 3): in fenchone (+), when the light is left-handed, more low-energy electrons (around the centre of the detector, electrons predominantly ionized by harmonic 3) are emitted in the backward direction than the forward direction. Switching the handedness of the light reverses the effect. The sign of the PECD switches when the electron energy increases, that is, as we move away from the centre of the detector.

Quantitative evaluation of the observed PECD requires Abel-inverting of the projected images. This data treatment procedure is described in detail in ref. 33. The PECD is shown in Fig. 4, which compares measurements performed in fenchone (+)

and (–). The data show a quasi-perfect mirroring between the two enantiomers, as expected from theory, showing the excellent signal-to-noise ratio that can be reached in an acquisition time of a matter of 15 min for each helicity. The PECD peaks at energies associated with the ionization of the two highest occupied molecular orbitals of fenchone (HOMO and HOMO-1). Interestingly, the responses of the two orbitals have opposite signs, which is consistent with synchrotron radiation measurements<sup>34</sup> and highlights the sensitivity of PECD to the ionized orbital. Harmonic 3, which is produced below the ionization threshold of SF<sub>6</sub>, produces a significant PECD. This harmonic could not be characterized in the optical polarimetry experiment because of the bandpass of the spectrometer, but the PECD measurement indicates that it is highly elliptical. The PECD changes sign between harmonic 3 and harmonics 5 or 7. This could be either due to the ionization dynamics of fenchone or to an opposite helicity of H3 and H5. These results demonstrate the possibility of performing high-quality PECD measurements with elliptical HHG, with the advantage of probing

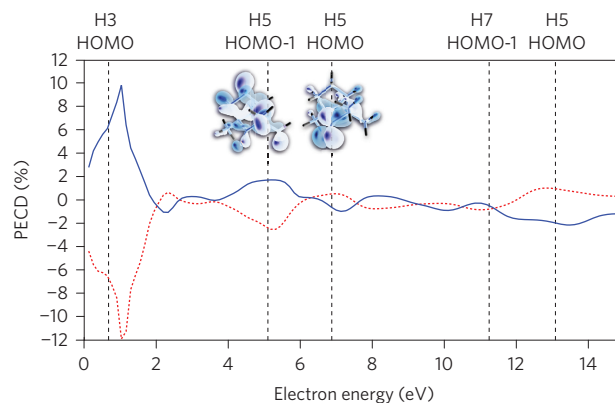


**Figure 4 | Photoelectron circular dichroism in fenchone.** PECD from fenchone (+) (red dots) and (–) (blue solid line) molecules ionized by high harmonics of a 400 nm fundamental pulse with  $\varepsilon_0 = 30\%$  as a function of electron energy. Three harmonics photoionize the system at 9.3 (harmonic 3), 15.5 (harmonic 5) and 21.7 eV (harmonic 7). The dichroism peaks at positions corresponding to the ionization of the two highest occupied molecular orbitals HOMO (ionization potential 8.6 eV) and HOMO-1 (10.4 eV).



several ionizing energies in the same measurement. Combined with a forthcoming purely circular ( $S_3 = 1$ ) synchrotron radiation calibration of the molecular chiroptical response at harmonic photon energies, this PECD measurement will allow the disentangling of Stokes parameters  $S_3$  (circular) and  $S_4$  (unpolarized radiation) of the harmonic emission. In a first approximation, assuming a fully polarized elliptical radiation with vertical ellipse axis, and a zero anisotropy parameter  $\beta$ , we can extract a value for the first-order Legendre polynomial coefficient  $b_1 = \text{PECD}/(2S_3)$  by using the ellipticities measured by optical polarimetry (Fig. 2). For the HOMO this gives  $b_1 \approx 4 \pm 2 \times 10^{-3}$  at a photon energy of 15.5 eV (harmonic 5) and  $b_1 \approx 1.1 \pm 0.5 \times 10^{-2}$  at a photon energy of 21.7 eV (harmonic 7). This is in decent agreement with synchrotron radiation measurements performed at neighbouring energies:  $b_1 \approx 7 \pm 5 \times 10^{-3}$  at 14 and 16 eV, and  $b_1 \approx 2 \pm 1 \times 10^{-2}$  at 22 eV (ref. 34).

By enabling the extension of the current frequency-resolved experiments carried out with synchrotron radiation to the time domain via pump-probe experiments, resonant HHG sources enable a very large avenue of research for 'femtochirality'. In particular, the transition states of enantioselective photochemical processes could be directly addressed by applying standard pump-probe femtochemistry methods. Other femtosecond probes of chirality in the gas phase have been demonstrated recently. Coulomb explosion imaging enables the absolute configuration of molecules to be determined<sup>35</sup>, but is restricted to small systems. Compared to multi-photon ionization<sup>36,37</sup>, XUV PECD has the advantage of being a universal direct ionization probe, involving no intermediate resonant state. Many photochemical processes could therefore be mapped out in the time domain by means of PECD, which is known to be extremely sensitive to static<sup>2</sup> and dynamical<sup>3</sup> molecular structures. Elliptical HHG also opens the path to attosecond metrology of circular dichroism. The temporal profile associated with the superposition of consecutive harmonics is an attosecond pulse train. Using an additional probe laser field enables resolving the phase of the molecular photoionization process<sup>15</sup>, giving access to attosecond time delays of the photoelectrons<sup>14</sup>. It will thus be possible to resolve the different photoionization times of photoelectrons emitted from a chiral molecule forward or backwards relative to the direction of the light propagation, thereby obtaining a unique insight into the fundamental dynamics of electrons in chiral potentials.

## Methods

The experiments were performed using the Aurore laser system at CELIA, which delivers 8 mJ, 25 fs, 800 nm pulses at 1 kHz. Frequency doubling was achieved using a 200- $\mu\text{m}$ -thick type I BBO crystal (4 mJ of 800 nm gives 1 mJ of 400 nm light). The polarization state of the fundamental radiation was shaped by rotating a broadband zero-order half-waveplate in front of a quarter-waveplate, which enabled the laser ellipticity  $\varepsilon_0$  to be varied while keeping the major axis of the ellipse fixed. The laser was focused by a thin 50 cm  $\text{SiO}_2$  lens into a vacuum chamber and interacted with a continuous jet (300  $\mu\text{m}$  nozzle) at 100 mbar or a static gas cell (3 mm long) filled at 5 mbar. Optical polarimetry using the two sources gave similar results. Note that  $\text{SF}_6$  has the advantage of being non-toxic, non-corrosive and gaseous at room temperature, with a high vapour pressure. The harmonic polarization state was characterized using an XUV polarizer consisting of three bare gold mirrors under  $75^\circ$ – $60^\circ$ – $75^\circ$  incidence, leading to a contrast of 5–20 between S and P polarizations for harmonics 5 to 9 of the 400 nm light. A second half-waveplate was used to rotate the laser polarization, which is equivalent to rotating the XUV polarizer, to record the Malus' law.

For the PECD experiment, a reservoir of enantiopure fenchone (Sigma Aldrich) at room temperature was connected through a microleak to a heated metallic nozzle (120  $^\circ\text{C}$ ) of 300  $\mu\text{m}$  diameter located 7 cm away from the interaction zone. The pressure in the interaction region was  $2 \times 10^{-6}$  mbar ( $5 \times 10^{-8}$  mbar background pressure).

Received 11 March 2014; accepted 27 November 2014;  
published online 22 December 2014

## References

- Böwering, N. *et al.* Asymmetry in photoelectron emission from chiral molecules induced by circularly polarized light. *Phys. Rev. Lett.* **86**, 1187–1190 (2001).
- Powis, I. Photoelectron circular dichroism in chiral molecules. *Adv. Chem. Phys.* **138**, 267–329 (2008).
- Garcia, G. A., Nahon, L., Daly, S. & Powis, I. Vibrationally induced inversion of photoelectron forward-backward asymmetry in chiral molecule photoionization by circularly polarized light. *Nature Commun.* **4**, 2132 (2013).
- Stohr, J. *et al.* Element-specific magnetic microscopy with circularly polarized X-rays. *Science* **259**, 658–661 (1993).
- Boeglin, C. *et al.* Distinguishing the ultrafast dynamics of spin and orbital moments in solids. *Nature* **465**, 458–461 (2010).
- Schoenlein, R. W. *et al.* Generation of femtosecond pulses of synchrotron radiation. *Science* **287**, 2237–2240 (2000).
- Čutić, N. *et al.* Vacuum ultraviolet circularly polarized coherent femtosecond pulses from laser seeded relativistic electrons. *Phys. Rev. ST Accel. Beams* **14**, 030706 (2011).
- Allaria, E. *et al.* Highly coherent and stable pulses from the FERMI seeded free-electron laser in the extreme ultraviolet. *Nature Photon.* **6**, 699–704 (2012).
- Le Déroff, L., Salières, P., Carré, B., Joyeux, D. & Phalippou, D. Measurement of the degree of spatial coherence of high-order harmonics using a Fresnel-mirror interferometer. *Phys. Rev. A* **61**, 043802 (2000).
- Hergott, J.-F. *et al.* Extreme-ultraviolet high-order harmonic pulses in the microjoule range. *Phys. Rev. A* **66**, 021801 (2002).
- Mahieu, B. *et al.* Full tunability of laser femtosecond high-order harmonics in the ultraviolet spectral range. *Appl. Phys. B* **108**, 43–49 (2012).
- Mairesse, Y. *et al.* High harmonic XUV spectral phase interferometry for direct electric-field reconstruction. *Phys. Rev. Lett.* **94**, 173903 (2005).
- Chini, M., Zhao, K. & Chang, Z. The generation, characterization and applications of broadband isolated attosecond pulses. *Nature Photon.* **8**, 178–186 (2014).
- Klünder, K. *et al.* Probing single-photon ionization on the attosecond time scale. *Phys. Rev. Lett.* **106**, 143002 (2011).
- Haessler, S. *et al.* Phase-resolved attosecond near-threshold photoionization of molecular nitrogen. *Phys. Rev. A* **80**, 011404(R) (2009).
- Lépine, F., Ivanov, M. Y. & Vrakking, M. J. J. Attosecond molecular dynamics: fact or fiction? *Nature Photon.* **8**, 195–204 (2014).
- Bauer, M. Femtosecond ultraviolet photoelectron spectroscopy of ultra-fast surface processes. *J. Phys. D* **38**, R253–R267 (2005).
- Vodungbo, B. *et al.* Polarization control of high order harmonics in the EUV photon energy range. *Opt. Express* **19**, 4346–4356 (2011).
- Budil, K. S., Salières, P., Perry, M. D. & L'Huillier, A. Influence of ellipticity on harmonic generation. *Phys. Rev. A* **48**, R3437–R3440 (1993).
- Antoine, P., Carré, B., L'Huillier, A. & Lewenstein, M. Polarization of high-order harmonics. *Phys. Rev. A* **55**, 1314–1324 (1997).
- Milšević, D. B., Becker, W. & Kopold, R. Generation of circularly polarized high-order harmonics by two-color coplanar field mixing. *Phys. Rev. A* **61**, 063403 (2000).
- Yuan, K.-J. & Bandrauk, A. D. Single circularly polarized attosecond pulse generation by intense few cycle elliptically polarized laser pulses and terahertz fields from molecular media. *Phys. Rev. Lett.* **110**, 023003 (2013).
- Fleischer, A., Kfir, O., Diskin, T., Sidorenko, P. & Cohen, O. Spin angular momentum and tunable polarization in high-harmonic generation. *Nature Photon.* **8**, 543–549 (2014).
- Smirnova, O. *et al.* Attosecond circular dichroism spectroscopy of polyatomic molecules. *Phys. Rev. Lett.* **102**, 063601 (2009).
- Zhou, X. *et al.* Elliptically polarized high-order harmonic emission from molecules in linearly polarized laser fields. *Phys. Rev. Lett.* **102**, 073902 (2009).
- Mairesse, Y. *et al.* High harmonic spectroscopy of multichannel dynamics in strong-field ionization. *Phys. Rev. Lett.* **104**, 213601 (2010).
- Yang, L. *et al.* Energy-dependent valence photoelectron spectra of  $\text{SF}_6$ : *ab initio* calculations and measurements. *J. Electron Spectrosc. Rel. Phenom.* **94**, 163–179 (1998).
- Ferré, A. *et al.* Multi-channel static and dynamical resonant high-order harmonic generation. *Nature Commun.* **5**, 5952 (2014).
- Chini, M. *et al.* Coherent phase-matched VUV generation by field-controlled bound states. *Nature Photon.* **8**, 437–441 (2014).
- Rabinovitch, K., Canfield, L. R. & Madden, R. P. A method for measuring polarization in the vacuum ultraviolet. *Appl. Opt.* **4**, 1005–1010 (1965).
- Ferré, A. *et al.* High-harmonic transient grating spectroscopy of  $\text{SF}_6$  molecular vibrations. *J. Phys. B* **47**, 124023 (2014).
- Falcão-Filho, E. L. *et al.* Scaling of high-order harmonic efficiencies with visible wavelength drivers: a route to efficient extreme ultraviolet sources. *Appl. Phys. Lett.* **97**, 061107 (2010).
- Nahon, L., Garcia, G. A., Harding, C. J., Mikajlo, E. & Powis, I. Determination of chiral asymmetries in the valence photoionization of camphor enantiomers by photoelectron imaging using tunable circularly polarized light. *J. Chem. Phys.* **125**, 114309 (2006).
- Powis, I., Harding, C. J., Garcia, G. A. & Nahon, L. A valence photoelectron imaging investigation of chiral asymmetry in the photoionization of fenchone and camphor. *Chem. Phys. Chem.* **9**, 475–483 (2008).

35. Pitzer, M. *et al.* Direct determination of absolute molecular stereochemistry in gas phase by Coulomb explosion imaging. *Science* **341**, 1096–1100 (2013).
36. Lux, C. *et al.* Circular dichroism in the photoelectron angular distributions of camphor and fenchone from multiphoton ionization with femtosecond laser pulses. *Angew. Chem. Int. Ed.* **51**, 5001–5005 (2012).
37. Janssen, M. H. M. & Powis, I. Detecting chirality in molecules by imaging photoelectron circular dichroism. *Phys. Chem. Chem. Phys.* **16**, 856–871 (2014).

### Acknowledgements

The authors thank R. Bouillaud and L. Merzeau for technical assistance, and M. Mairesse for mechanical supplies. The authors acknowledge financial support from the Conseil Régional d'Aquitaine (20091304003 ATTOMOL and COLA 2 no. 2.1.3-09010502), l'Agence Nationale pour la Recherche (ANR-14-CE32-0014 MISFITS and ANR-14-CE32-0010 XTASE), the European Union (Laserlab-Europe II no. 228334 and EU-FP7 284464) and the RTRA Triangle de la Physique (Attocontrol).

### Author contributions

C.H. built the VMIS. F.B., D.D. and S.P. operated the laser system. A.F., E.M., V.B. and Y.M. built the high-harmonic beamline. A.F., M.D., A.C., R.G., L.M., D.S., S.W., T.R., V.B. and Y.M. carried out the measurements. A.F. and Y.M. analysed the optical polarimetry measurements. G.A.G. and L.N. inverted the VMIS images and extracted and rationalized the PECD data. B.P. performed the theoretical calculations. Y.M. designed the manuscript. All authors contributed to the interpretation of the data and writing of the manuscript.

### Additional information

Supplementary information is available in the [online version](#) of the paper. Reprints and permissions information is available online at [www.nature.com/reprints](http://www.nature.com/reprints). Correspondence and requests for materials should be addressed to Y.M.

### Competing financial interests

The authors declare no competing financial interests.